Electronic Supplementary Material (ESI) for Nanoscale Advances.

Ultrahigh Photo-Stable All-Inorganic Perovskite Nanocrystals and Their Robust Random Lasing

Liuli Yang[a], Ting Wang[a], Qiuhong Min[a], Chaojie Pi[a], Fan Li[b], Xiao Yang[b], Kongzhai Li[c], Dacheng Zhou[a], Jianbei Qiu[a] , Xue Yu[a,*] , Xuhui Xu[a,*]

[a] Faculty of Materials Science and Engineering, Kunming University of Science and Technology, Wenchang Road. Kunming, 650093, China

[b] Department of Materials Science and Engineering, Nanchang University, 999 Xuefu Avenue, Nanchang 330031, China.

[c] State Key Laboratory of Complex Nonferrous Metal Resources Clean Utilization, Kunming University of Science and Technology, Kunming 650093, China

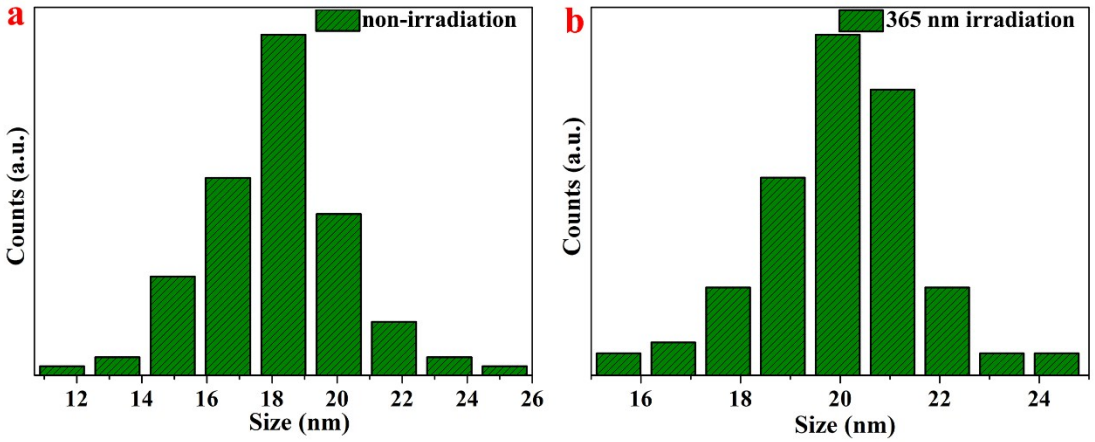

Figure S1. Size distributions of non- (a) and 365 nm-(b) irradiated $CsPbBr_3$ NCs.

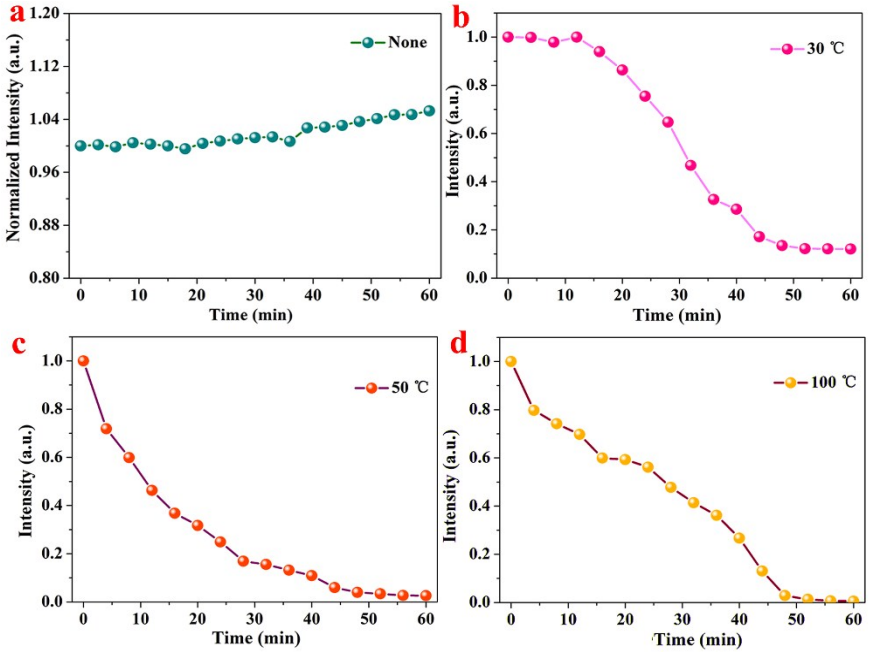

Figure S2. The green emission intensity of the sample under the excitation of 365 nm measured at room

temperature (a), 30°C (b), 50°C (c) and 70°C (d) by prolonging the irradiation time. The emission intensity is recorded after the Cs_4PbBr_6 NCs immersed in water for 1min.

More drastic decrease of the emission intensity indicates that thermal energy deteriorates the green emission rather than promote the transformation to obtain $CsPbBr_3$ NCs.

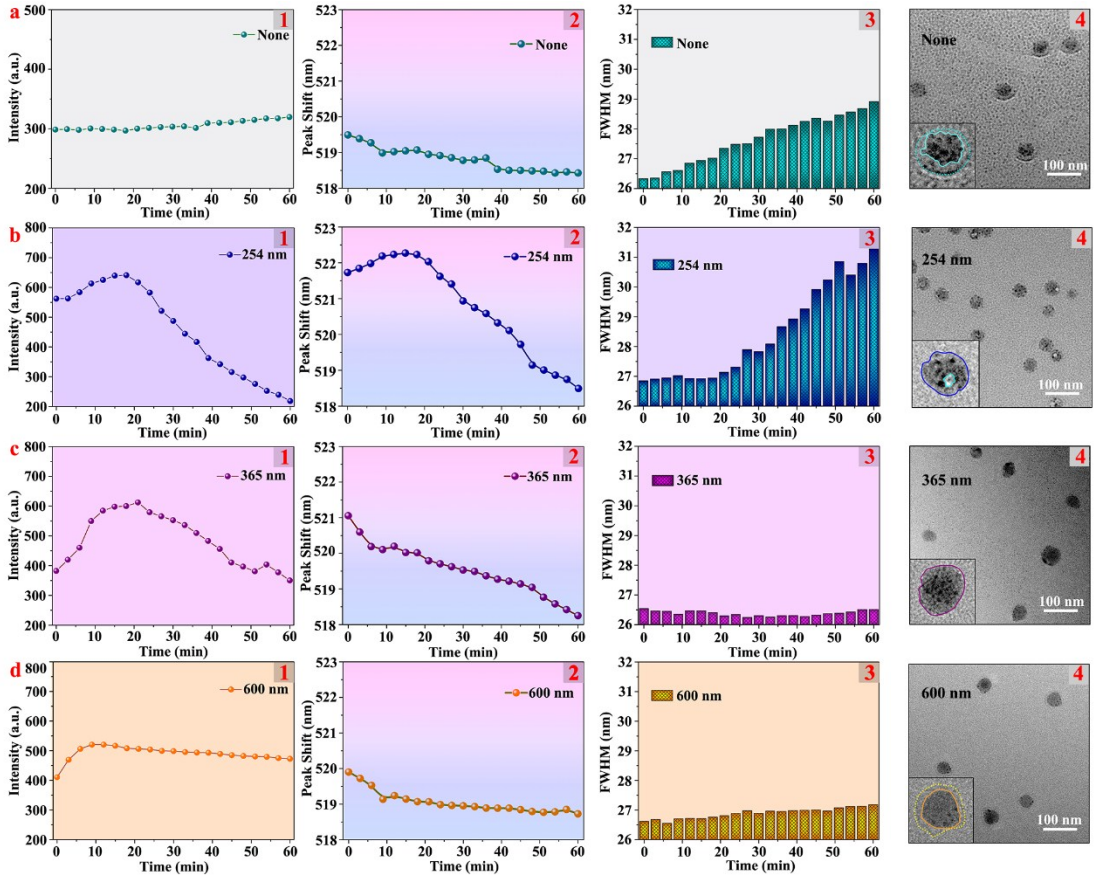

Figure S3. The emission intensity (a1-d1), peak location (a2-d2), and full-width-at-half-maximum (FWHM) (a3-d3) of the sample recorded with the excitation of 365 nm under non, 254, 365, and 600 nm-irradiation within 60 min, respectively, and TEM images (a4-d4) of the sub-$CsPbBr_3$ NCs after 20 min with the irradiation of different wavelength, and the inset is the TEM image of the corresponding single-particle. The emission intensity is recorded after the Cs_4PbBr_6 NCs immersed in water for 1 min.

The improvement of the green emission intensity is observed in Figure S3 (b1-d1) during the initial 20 min compared with the sample without irradiation involved (Figure S3a1), which indicates that an accelerated phase transformation from Cs_4PbBr_6 NCs to luminescent $CsPbBr_3$ NCs is realized with the intervention of 254, 365 and 600 nm light irradiation. During the phase transformation process, the NCs undergo size reduction and structural reorganization. As shown in Figure S3 (a2-d2) a more drastic red-shift of the peak location is observed under 254 nm-irradiation within 20 min compared to other irradiation conditions, which may be due to the destruction of the NCs structure during the structural reorganization.[1] The blue-shift of the peak location in FigureS3 a2, c2 and d2 is mainly attributed to the size reduction.[2] What's more, the increase of the FWHM when the sample irradiated by 365 nm within 20 min is minimal as shown in Figure S3 (a3-d3), indicating that the structural destruction is minimal.[3] TEM images shown in Figure S3 (a4-d4) indicate that CsBr NCs are precipitated on the surface of these samples after 20 min. The inset of Figure S3a4 reveals that the sample without irradiation exhibits a thick layer of

organic ligands coating on the surface. However, organic ligands on the surface of the sample with 254, 365 nm irradiation is not obviously observed as shown in the insets of Figure S3 (b4-c4), while an organic layer on the surface of the sample treated with 600 nm-irradiation is detected as the inset of Figure S3d4. The existence of organic ligands is believed to impede the contact of water and nanocrystals and detrimental to the phase transformation. Different from the corresponding sample with 365 nm-irradiation, the surface of the sample with 254 nm-irradiation is obviously damaged, indicating the damage of the structure as shown in Figure S3b4, which is consistent with the observation of redshift of sample Figure S3b2. Combined with less organic ligands and no surface damage, 365 nm is employed as the optimal irradiation to accelerate the phase transformation.

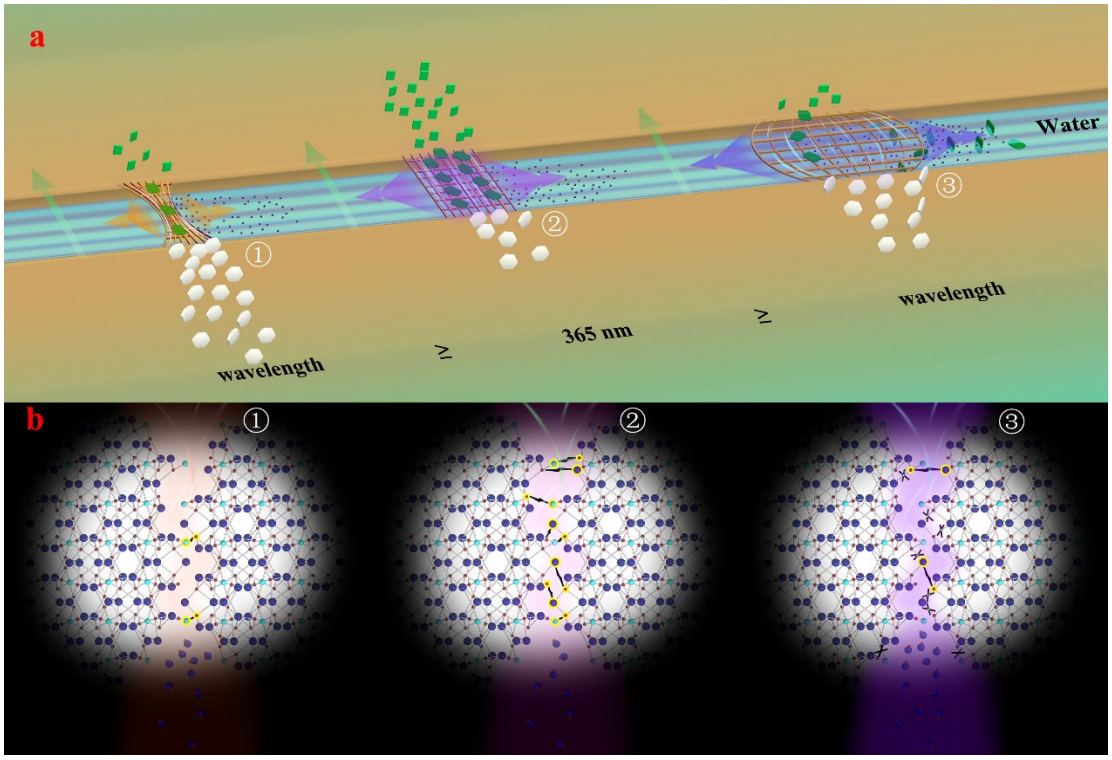

Figure S4. Schematic (a) and mechanism (b) diagram of the proposed phase transformation process under different irradiation condition.

A few atoms could be rearranged with the photon energy of 600 nm-irradiation in the small area (Figure S4a1 and b1), while all the atoms in a large area are rearranged under 365 nm-irradiation, which greatly accelerate the transformation (Figure S4a2-b2). Moreover, although 254 nm light provides enough energy to rearrange atoms, the relative higher photon energy destroys the structure as well, as shown in Figure S4 (a3-b3).

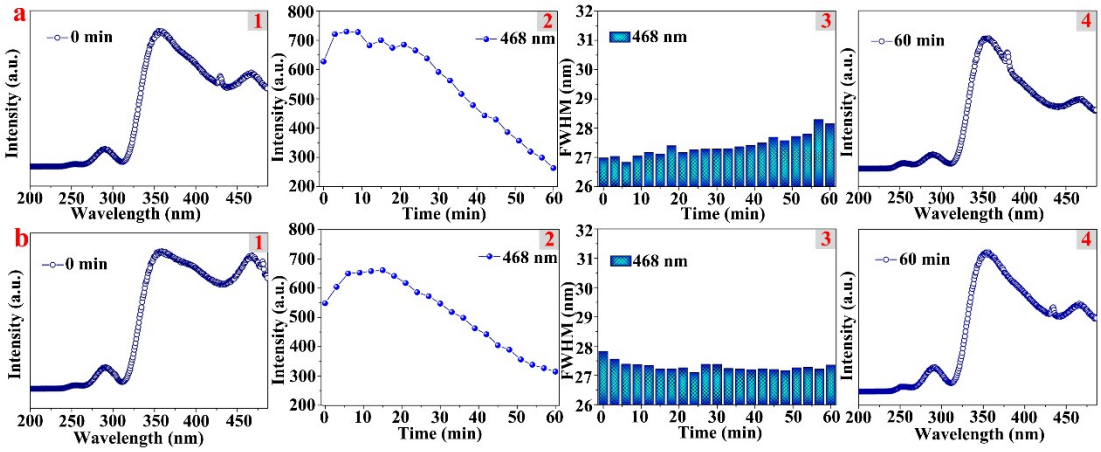

Figure S5. Photoluminescence excitation (PLE) monitored at 520 nm (a1 and b1), time-dependent emission intensity obtained under the excitation of 365 nm (a2 and b2), and time-dependent FWHM under irradiation at 468 nm (a3 and b3), PLE under irradiation at 468 nm for 60 min (a4 and b4), respectively. Figure S5a and S5b is recorded immediately and after 1 min for Cs_4PbBr_6 NCs immersed in water, respectively.

Clearly, when 468 nm is not the optimal absorption band (Figure S5a1), the emission intensity of the sample increases at first and then decreases (Figure S5a2), and the FWHM increases with the prolonged 468 nm-irradiation time (Figure S5a3). In contrast, when 468 nm is the optimal absorption band (Figure S5b1), the emission intensity of the sample exhibits similar change trend (Figure S5b2), but the FWHM of the sample does not increase with the increase of 468 nm-irradiation time (Figure S5b3). These results are consistent with as the observation of the sample under 365 nm-irradiation. It should be noticed that 365nm is the optimal absorption band (Figure S5a3 and b3), although the PLE spectrum of the sample changes.

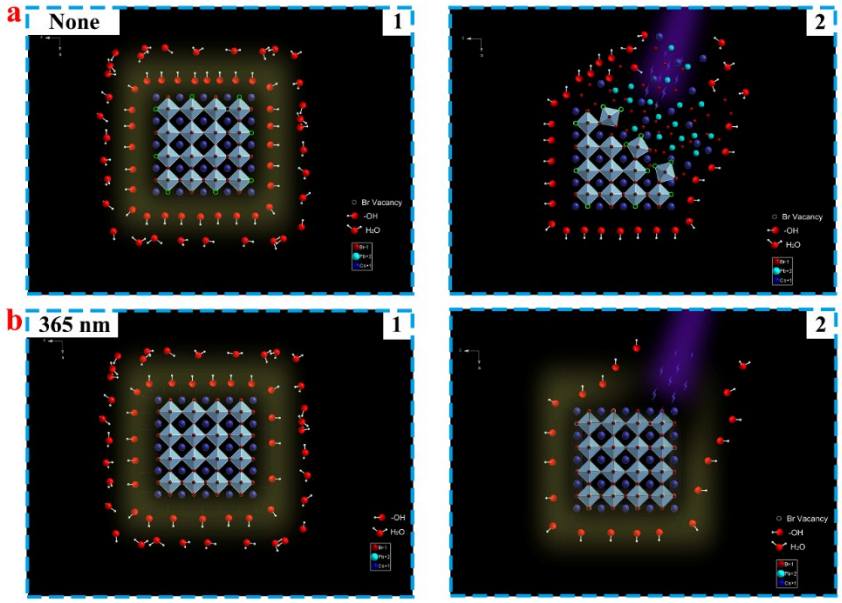

Figure S6. Diagrams of the mechanisms of water stability (a1, b1) and radiation stability (a2, b2) corresponding to Figure 3g and 3h.

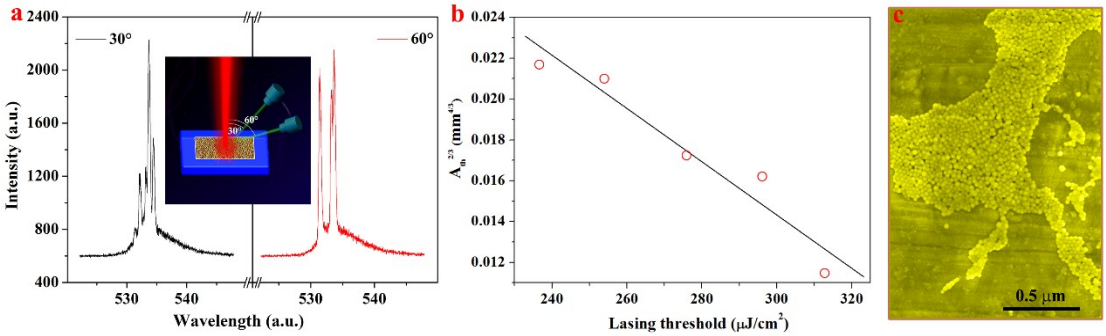

Figure S7. Lasing spectra (a) are recorded from two directions: 30° and 60 °. Variation of the lasing threshold as a function of the excitation area on a logarithmic scale (b). The corresponding SEM images of the samples after excited by femtosecond laser beam with the pump density of $1.5P_{th}$ (8.6×10^7 excitation cycles) (c).

Category / Area ratio / Wavelength	Pb-O $_{left}$	Pb-Br $_{left}$	Pb-O $_{right}$	Pb-Br $_{right}$
None	0.69	1	0.51	0.75
254 nm	0.84	1	0.63	0.74
365 nm	0.36	1	0.27	0.74
600 nm	0.67	1	0.50	0.74

Table S1. Summary of components of non-irradiated samples and 365 nm-irradiated samples.

REFERENCES

1. Mićić, O. I., Sprague, J., Lu, Z., Nozik, A. J., (1996). Highly efficient band−edge emission from InP quantum dots. *Appl. Phys. Lett.* **1996,** 68, (22), 3150-3152.

2. Wen, Z.; Zhai, W.; Liu, C.; Lin, J.; Yu, C.; Huang, Y.; Zhang, J.; Tang, C., (2019). Controllable synthesis of $CsPbI_3$ nanorods with tunable photoluminescence emission. *RSC Adv.* **2019,** 9, (43), 24928-24934.

3. Luo, J.; Wang, X.; Li, S.; Liu, J.; Guo, Y.; Niu, G.; Yao, L.; Fu, Y.; Gao, L.; Dong, Q.; Zhao, C.; Leng, M.; Ma, F.; Liang, W.; Wang, L.; Jin, S.; Han, J.; Zhang, L.; Etheridge, J.; Wang, J.; Yan, Y.; Sargent, E. S.; Tang, J., Efficient and stable emission of warm-white light from lead-free halide double perovskites. *Nature* **2018,** 563, 541–545.